Progress In Electromagnetics Research C, Vol. 123, 17–26, 2022

Array Pattern Restoration under Defective Elements

Jafar R. Mohammed* and Ahmed J. Abdulqader

Abstract—The defective array elements which are unavoidable due to the long full-time antenna system operation directly affect its radiation pattern, sidelobe level, directivity, and the system performance. Therefore, reducing these undesirable effects is a main interest in designing such arrays in practice. In this paper, a partially compensating method based on the genetic optimization algorithm is proposed to mainly reduce those undesirable effects of the defected elements. Unlike the existing fully compensating methods where all of their active elements were optimized to compensate for the effects of the defected elements, the proposed method optimizes the excitation weights of some optimally selected active-elements. Thus, the whole array elements do not need to be redesigned again as in the case of the fully compensating methods. This greatly simplifies the design implementation of these arrays. Moreover, a very large defective percentage ranging from 5% up to 50% has been considered to demonstrate the effectiveness of the proposed method. Furthermore, the drawback effects of the randomly failing elements at the array center have been highlighted, and some suggestions have been provided.

1. INTRODUCTION

Defective elements in an array cause unexpected pattern distortion and an increase in the sidelobe level which leads to more waste of the radiation energy in undesired directions and cause interference. Therefore, it is necessary to restore the desired radiation pattern under such unavoidable failed situations. In the literature, a very few of analytical methods were found to deal with this problem, for example see [1], and only a limited number of the numerical methods have been devised to redesign the whole defected array by recalculating all the excitation weights of the active elements to compensate the weights of the defective elements and restore the desired radiation pattern. These methods are known as fully compensating methods. Peters [2] proposed a conjugate gradient method to recalculate the amplitude and phase excitations of all active (i.e., none failed) elements to minimize the sidelobe pattern distortion. Then Yeo and Lu [3] used a genetic algorithm (GA) while Grewal et al. [4] used a firefly optimization algorithm to redesign all elements of the defected array. Some other researchers [5, 6] used only a part of active array elements to restore the desired array pattern. In [5], the authors used particle swarm optimization (PSO) to address the limits of compensation in a failed array, while in [6] the authors used a GA to find the minimum number of adjustable active elements to compensate the defective elements. Another method based on the hardware replacement was suggested by Mailloux [7] where the signals from the defected elements were replaced in the digital beamformer circuit. However, the hardware replacement method is generally time-consuming which may be not a good choice for many practical applications. In [8], Keizer extended his newly suggested method based on an iterative fast Fourier transform to deal with the problem of element failure correction. In all of those aforementioned methods, it is required to readjust (or redesign) the excitation weights of all or most of the active elements which are practically complex and time consuming. Moreover, they are only considered a very limited number of defective elements that are usually located randomly on the array sides and

Received 11 June 2022, Accepted 8 August 2022, Scheduled 19 August 2022
* Corresponding author: Jafar Ramadhan Mohammed (jafar.mohammed@uoninevah.edu.iq).
The authors are with the College of Electronics Engineering, Ninevah University, Mosul 41002, Iraq.

not on the array center [9, 10]. As a matter of fact, the central array elements usually have the largest excitation weights which make their compensation difficult when they are facing faults.

In this paper, a partially compensating method based on GA is suggested to reduce the effects of the defective elements. The array elements are first divided into three types based on their excitation weights. The first type is the defective elements which are considered randomly across the array, and their magnitude weights are zero, while the other type is compensating elements which are adaptive, and their excitation weights are re-updated by means of genetic optimization. The last type is the fixed elements in which their magnitudes are fixed according to a certain array taper. By this way, not all the active array elements need recalculation as in the existing fully compensating methods, and instead only the compensating elements are optimally optimized to correct the damaged pattern. GA was used to find the optimum number of compensating elements and their excitation weights without redesigning the whole array elements. A specific cost function has been formulated to correct the damaged pattern by iteratively minimizing the difference between the obtained SLL and the desired one. Moreover, the effects of the failing elements at the array center have been highlighted, and some suggestions have been provided.

2. THE DEFECTED ARRAYS

In this section, fully and partially compensating methods are introduced.

2.1. Fully Compensating Elements

To proceed with this method, first suppose a uniform linear array of $2N$ isotropic elements placed symmetrically about the x-axis with uniform inter-element spacing of $d = 0.5\lambda$. The normalized array factor of such an antenna array as a function of elevation angle θ can be expressed as [11]:

$$AF(\theta) = \sum_{n=1}^{N} a_n \cos\left(\frac{2n-1}{2}\, kd \sin\theta + p_n\right) \tag{1}$$

where parameters a_n and p_n are the amplitude and phase weightings of the nth elements, respectively. The wave number k is equal to $\frac{2\pi}{\lambda}$, and λ is the wavelength. For simplicity, the amplitude-only weighting approach is used; thus, the phases are set to zero. In the defected array, the inter-element spacing between active elements will be changed and may become nonuniform according to how many defective elements are presented. From (1), the amplitude weights of the randomly defected elements, a_n, will be set to zero, while all the other weights will be optimized to provide the required compensation for pattern correction.

2.2. Partially Compensating Elements

In this approach, the number of compensated (or optimized) elements is restricted to only specific subset elements instead of all array elements. The central elements are assumed to have fixed weights, while the compensating elements are assumed to be located near the edges of the array aperture. This is mainly because the edge elements have the highest effect on the array pattern alteration [12]. The locations of the defective elements are assumed to be random across the array aperture. To proceed, assume that a subset of N_c out of N total active elements on each side of the linear array is made variable and subject to the optimization process.

The remaining number of the central active elements, $N - N_c$, keep their magnitude excitations fixed according to the used taper. Note that the absence of the last element in each side of the array reduces the array aperture and consequently results in a wide beam width of the array pattern. To prevent such an issue, it is assumed that the last element on each side of the array is always active and intact so that the array aperture is preserved. The total far-field radiation pattern of these two subsets (i.e., compensated subset array of N_c adaptive elements and a tapered subset array of $N - N_c$ elements) can be written as:

$$AF(\theta) = \underbrace{\sum_{n=1}^{N-N_c} a_n \cos\left(\frac{2n-1}{2} kd \sin\theta\right)}_{\text{Central fixed elements}} + \underbrace{\sum_{m=N-N_c+1}^{N} b_m \cos(kd_m \cos\theta)}_{\text{Compensating elements}} \tag{2}$$

For magnitude-only weighting method, the values of b_m are only optimized while the values of a_n are fixed according to the used taper. First, the number of defective elements should be given in advance, but their locations should be randomly selected. Then the GA is used to find the number of compensating elements, N_c, and their amplitude weights, b_m, such that the obtained radiation pattern with the defected elements has a sidelobe level as close as possible to the desired level. To solve such an optimization problem, a cost function is formulated as follows:

$$\text{Cost} = \frac{1}{S} \sum_{s=1}^{S} \left[|AF(\theta_s)| - \text{SLL}_d(\theta_s)\right]^2 \tag{3}$$

where S is the total number of the sample points, and SLL_d is the desired sidelobe level. According to (3), the obtained array pattern at the sidelobe region (i.e., $|\theta| \geq$ FNBW where FNBW represents the first null-to-null beam width) and the desired sidelobe level are both vertically and equally sampled into S points. For each sample point, the difference between the obtained and the desired sidelobe levels is computed. If the magnitudes of the obtained SLLs are above the desired ones, then the compensating weights should be iteratively updated until they become below or as close as possible to the desired ones. This iterative change contributes to minimization of the cost which is actually the error between the obtained and desired sidelobe patterns.

3. SIMULATION RESULTS

In all examples, a symmetric linear array of $2N = 40$ radiating elements was considered. The maximum number of iterations is set to 150, and the population size is set to 50. The other parameters of the genetic algorithm were chosen as follows: the crossover was single point; selection was roulette; the mutation rate was 0.15; finally, the mating pool was chosen to be 4. The lower and upper bounds of the amplitudes of the compensating elements were chosen between 0 and 1. All the optimization processes were implemented on a laptop with windows 10 Pro 64 bit operating system, processor type Intel (R) Core TM i5, CPU @ 1.6 GHz 1.8 GHz and memory size of 4 G byte RAM.

In the first example, a fully compensated approach, where all of the active elements are optimized, is considered and applied to magnitude-only weighting method to obtain an SLL as close as possible to the desired one which is set at $\text{SLL}_d = -30$ dB and, at the same time, to place two symmetric wide nulls centered at $\theta = \pm 40°$ each with a width equal to $\theta = 10°$. The number of randomly defective elements is assumed to be 4 on each side of the array (i.e., the defective percentage is 20%). The results of the original Taylor excited array pattern, damaged and the restored array patterns are shown in Fig. 1. The corresponding excitation weights for these three patterns are also shown in Fig. 1. The restored patterns have exactly met the desired SLL and the controlled nulls. However, the number of compensating elements was 16 among a total of 20 elements on each side of the array which is relatively large.

In the second example, the same results of example 1 were obtained with a partially compensated approach for only a number of optimized elements equal to $N_c = 11$. For comparison purposes, the number of the defective elements, the desired SLL, and the controlled nulls were all set as in the previous example. The results are shown in Fig. 2. It can be seen that the same results can be obtained with less number of the optimized elements.

In the third example, the variation in the number of defective elements on the performance of the partially compensated approach is investigated. Table 1 and Fig. 3–Fig. 5 show the results. From Table 1, it can be seen that the performances of both damaged and restored patterns in terms of taper efficiency, directivity, peak SLL, and FNBW are all getting worse with an increase in the number of randomly defective elements. However, the peak SLL of the restored patterns for all cases including the case of defective percentage 50% is below -21 dB. Also, these figures show that the main beam widths

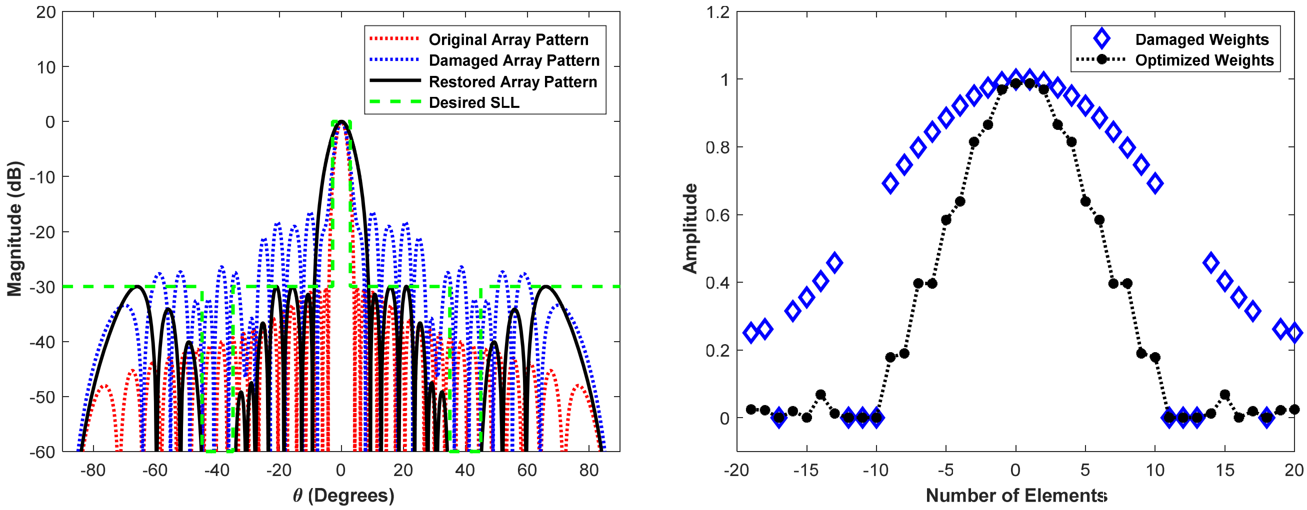

Figure 1. The results of fully compensated approach for 8 defective elements, 32 compensating elements, $\mathrm{SLL}_d = -30\,\mathrm{dB}$ and two wide nulls.

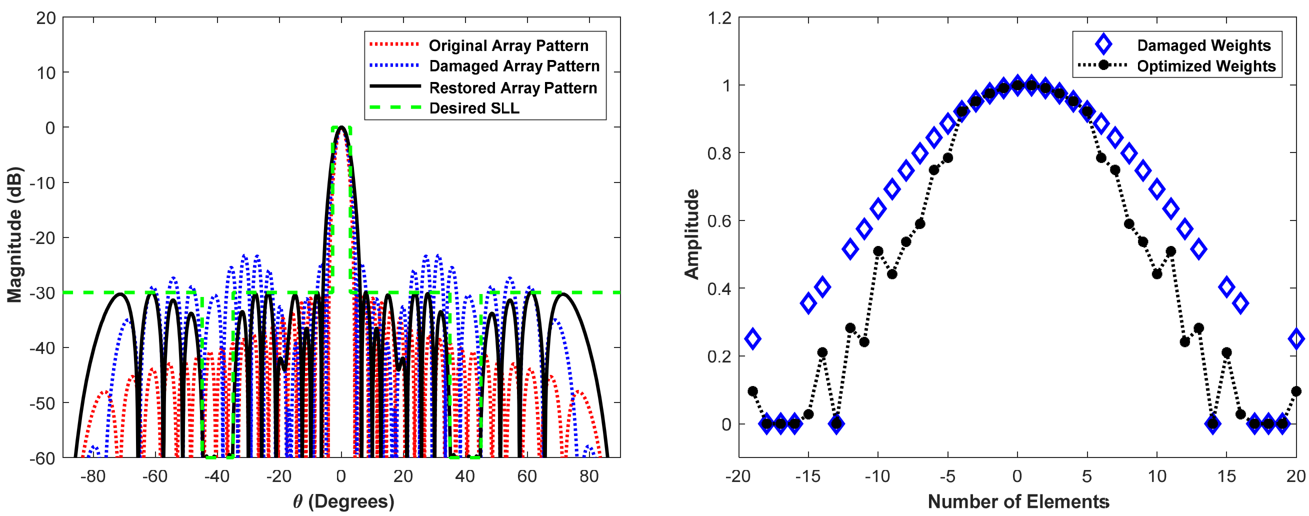

Figure 2. The results of partially compensated approach for 8 defective elements, 10 central fixed elements, 22 compensating elements, $\mathrm{SLL}_d = -30\,\mathrm{dB}$ and two wide nulls.

of the restored patterns are gradually broadened with an increased number of defective elements. This is mainly because the amplitude excitations of the compensating elements get narrower which directly results in broader main beams.

In order to show the versatility of the proposed method, it has also been applied to a uniformly excited array. The results of 4 defective elements on each side of the array are shown in Fig. 6. The performance measurements of the original, damaged, and restored patterns are shown in Table 2. Note that the obtained SLL of the restored pattern is below $-30\,\mathrm{dB}$.

Some advantages of the proposed method compared to other existing methods are highlighted in Table 3.

Next, the effect of the defective elements at the array center is considered. As mentioned earlier, the central elements possess the largest amplitude weights. Thus, they have more impact on the array pattern distortion and cannot be easily compensated by optimizing other elements. It is worth mentioning that the central defected elements have not been investigated before by any other researchers. Fig. 7 and Fig. 8 show the results for two cases of 4 and 8 randomly central defective elements. Table 4

Table 1. Performance measures as a function of the number of defective elements in the partially compensated approach.

Performances	Original Taylor Pattern	Restored Pattern										
		Number of random defective elements on each side of the array										
			1	2	3	4	5	6	7	8	9	10
Taper Efficiency	0.85	Damaged	0.81	0.77	0.75	0.70	0.63	0.6	0.57	0.52	0.49	0.47
		Restored	0.70	0.61	0.71	0.52	0.4	0.4	0.39	0.39	0.39	0.39
Directivity (dB)	26.77	Damaged	26.4	26.1	25.8	25.29	24.4	24.1	23.8	22.7	22.2	21.7
		Restored	25.1	24.0	25.2	22.60	20.4	20.3	20.1	20.2	20.1	20
Peak SLL (dB)	−30	Damaged	−23	−24	−26	−21	−15	−16	−17	−13	−13	−14
		Restored	−30	−30	−30	−30	−21	−21	−21	−21	−21	−21
FNBW (deg.)	8	Damaged	8.8	9	9	10.6	15	14.6	14.6	14.4	14.2	13.3
		Restored	10.1	11.4	10	14	16.4	16.4	16.6	16.6	16.8	16.6
Amplitude Weights	$\lvert a_n^T \rvert = \lvert a_{-n}^T \rvert$	$\lvert a_n^D \rvert = \lvert a_{-n}^D \rvert$										
	0.2507	Restored Weights	0.04	0.00	0.11	0.00	0.00	0.00	0.00	0.00	0.00	0.00
	0.2617		0.07	**0**	**0**	**0**	0.07	0.06	**0**	0.06	**0**	**0**
	0.2833		0.11	0.02	0.19	0.00	0.04	0.02	**0**	**0**	0.06	**0**
	0.3150		0.10	0.07	**0**	0.01	0.04	**0**	0.00	0.00	**0**	**0**
	0.3556		0.23	0.08	0.28	**0**	**0**	**0**	**0**	**0**	**0**	**0**
	0.4037		0.23	0.15	**0**	0.13	**0**	0.00	0.02	**0**	**0**	**0**
	0.4577		0.39	0.19	0.38	**0**	0.00	**0**	**0**	**0**	**0**	**0**
	0.5155		**0**	0.33	0.48	**0**	0.00	0.00	0.00	**0**	**0**	**0**
	0.5751		0.54	**0**	0.43	0.24	**0**	**0**	**0**	**0**	**0**	**0**
	0.6346		0.50	0.48	0.49	0.31	**0**	**0**	**0**	**0**	**0**	**0**
	0.6924		0.64	0.49	0.63	0.28	**0**	**0**	**0**	**0**	**0**	**0**
	0.7473		0.71	0.64	0.68	0.51	0.29	0.32	0.31	0.31	0.24	0.30
	0.7982		0.79	0.68	0.77	0.44	0.29	0.29	0.30	0.28	0.31	0.31
	0.8446		0.80	0.77	0.75	0.70	0.56	0.54	0.52	0.53	0.52	0.52
	0.8860		0.89	0.84	0.84	0.73	0.53	0.56	0.55	0.55	0.52	0.53
	0.9219		**0.92**	**0.92**	**0.92**	**0.92**	**0.92**	**0.92**	**0.92**	**0.92**	**0.92**	**0.92**
	0.9517		**0.95**	**0.95**	**0.95**	**0.95**	**0.95**	**0.95**	**0.95**	**0.95**	**0.95**	**0.95**
	0.9750		**0.97**	**0.97**	**0.97**	**0.97**	**0.97**	**0.97**	**0.97**	**0.97**	**0.97**	**0.97**
	0.9909		**0.99**	**0.99**	**0.99**	**0.99**	**0.99**	**0.99**	**0.99**	**0.99**	**0.99**	**0.99**
	0.9990		**0.99**	**0.99**	**0.99**	**0.99**	**0.99**	**0.99**	**0.99**	**0.99**	**0.99**	**0.99**

Table 2. Performance measures for uniformly excited array with 8 defective elements.

Performance	Original Pattern	Damaged Pattern	Restored Pattern
Taper Efficiency	1	0.8	0.4
Directivity (dB)	28.20	27.02	20.38
Peak SLL (dB)	−13.2	−15.0	−30.0
FNBW (deg.)	5.6	6.2	16
Amplitude Weights	[1, 1, 1, 1, 1, 1, 1, 1, 1, 1, 1, 1, 1, 1, 1, 1, 1, 1, 1, 1]	[1, 1, 0, 1, 1, 0, 1, 1, 1, 0, 0, 1, 1, 1, 1, 1, 1, 1, 1, 1]	[0.0000, 0.0686, 0, 0.0003, 0.0000, 0, 0.0048, 0.0000, 0.0000, 0, 0, 0.3406, 0.3233, 0.5979, 0.6216, 1, 1, 1, 1, 1]

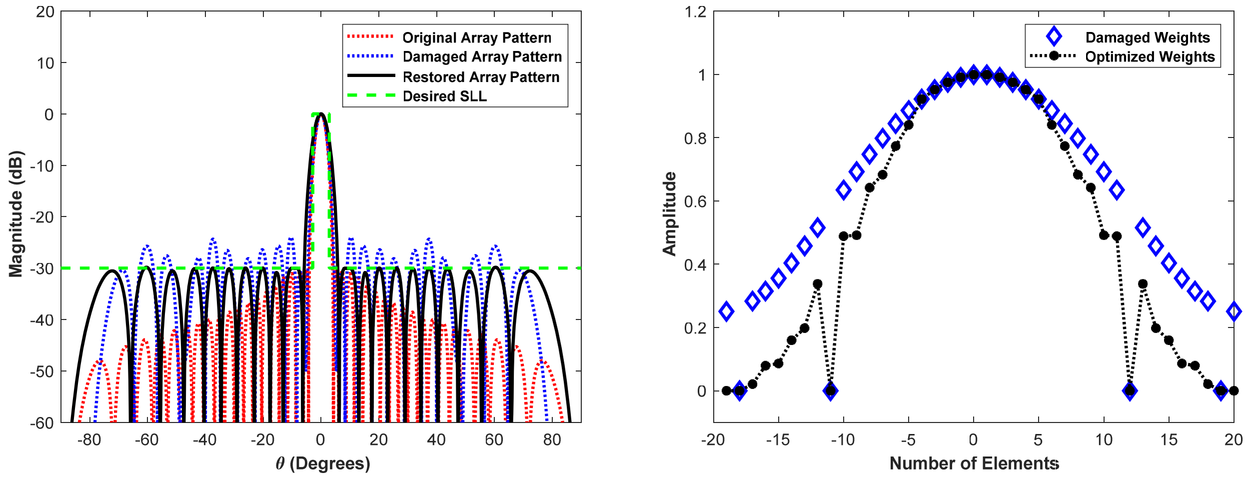

Figure 3. The original, damaged and the restored array patterns and their corresponding amplitude weights for 4 defective elements, 26 compensating elements, and 10 central fixed elements.

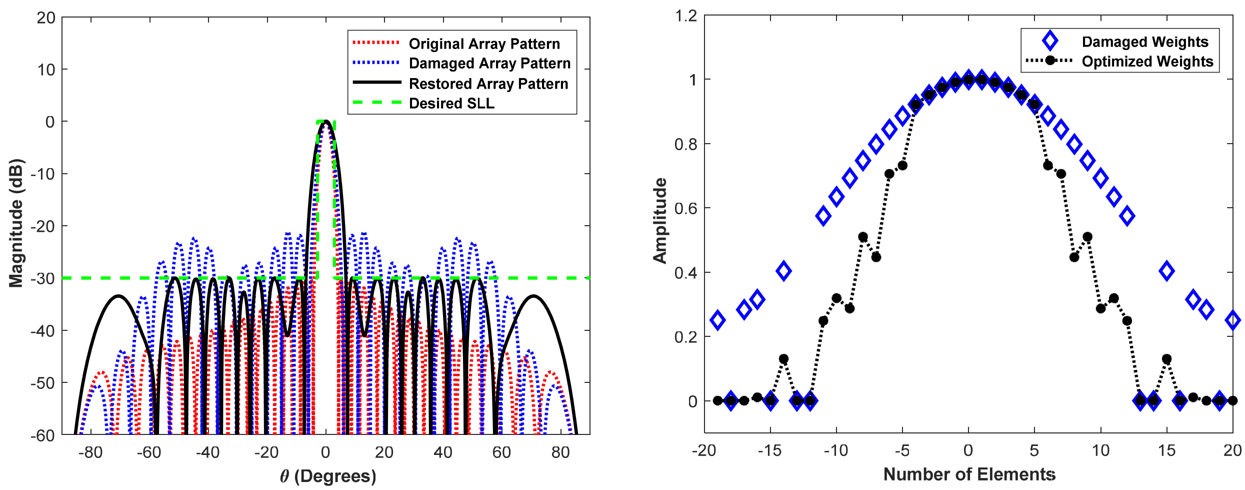

Figure 4. The original, damaged and the restored array patterns and their corresponding amplitude weights for 8 defective elements, 22 compensating elements and 10 central fixed elements.

Table 3. Comparative between different methods.

Methods	Max. defective percentage	Fully or Partially optimization scheme	Obtained SLL	Relative execution time	Redesigning weights (i.e., feeding network complexity)
The method in [3]	18.75%	Fully	−35.2 dB	High	All elements
The method in [4]	31.25%	Fully	−35 dB	High	All elements
The method in [5]	30%	Partially	−30 dB	Moderate	Part of elements
The method in [6]	6%	Partially	−22.4 dB	Moderate	Part of elements
This method	50%	Partially	−21 dB	Moderate	Only compensating elements

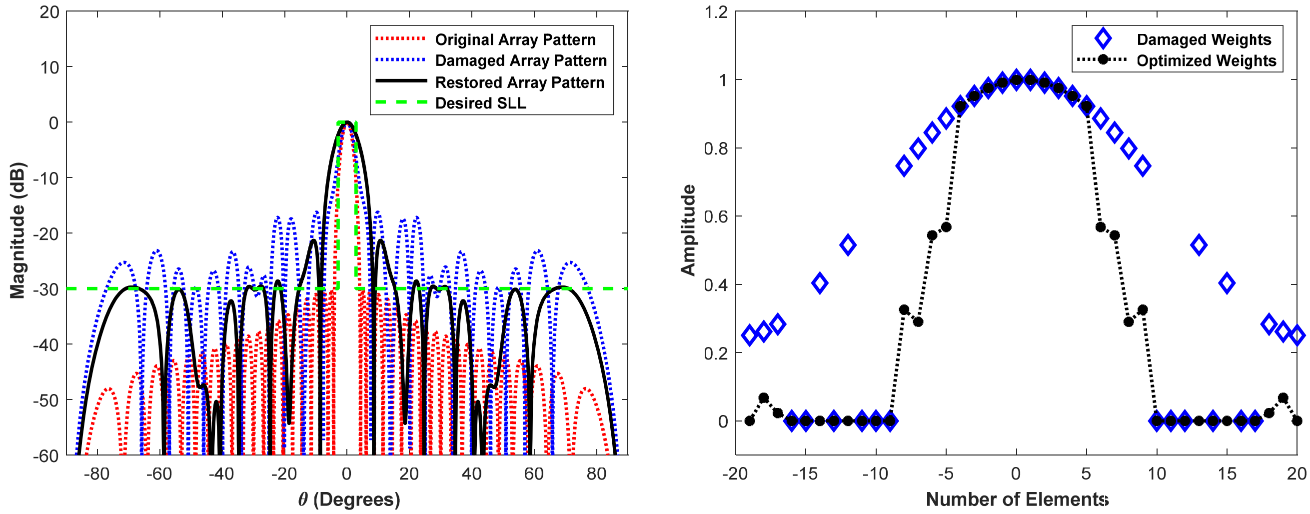

Figure 5. The original, damaged and the restored array patterns and their corresponding amplitude weights for 12 defective elements, 18 compensating elements, and 10 central fixed elements.

Table 4. Performance measures for central defective elements approach.

Performance	Original Pattern	4 Central Defective Elements		8 Central Defective Elements	
		Damaged Pattern	Restored Pattern	Damaged Pattern	Restored Pattern
Taper Efficiency	0.85	0.76	0.68	0.67	0.68
Directivity (dB)	26.77	26.61	27.35	26.66	27.04
Peak SLL (dB)	−30	−16.2	−17	−16.6	−8.2
FNBW (deg.)	7	6.6	5.2	5.8	4.9
Amplitude Weights	0.2507	0.2507	0.1626	0.2507	0.2615
	0.2617	0.2617	0.2424	0.2617	0.2468
	0.2833	0.2833	0.3023	0.2833	0.3973
	0.3150	0.3150	0.3105	0.3150	0.3817
	0.3556	0.3556	0.3866	0.3556	0.4752
	0.4037	0.4037	0.3421	0.4037	0.5392
	0.4577	0.4577	0.4608	0.4577	0.4704
	0.5155	0.5155	0.3160	0.5155	0.7019
	0.5751	0.5751	0.6757	0.5751	0.3952
	0.6346	0.6346	0.2804	0.6346	0.8572
	0.6924	0.6924	0.8109	0.6924	0.2722
	0.7473	0.7473	0.2095	0.7473	0.9049
	0.7982	0.7982	0.9306	0	0
	0.8446	0	0	0.8446	0.8314
	0.8860	0.8860	1.0000	0	0
	0.9219	0.9219	0.2588	0.9219	0.7103
	0.9517	0.9517	0.9847	0	0
	0.9750	0	0	0.9750	0.4640
	0.9909	0.9909	0.8706	0.9909	0.2562
	0.9909	0.9909	0.5368	0	0

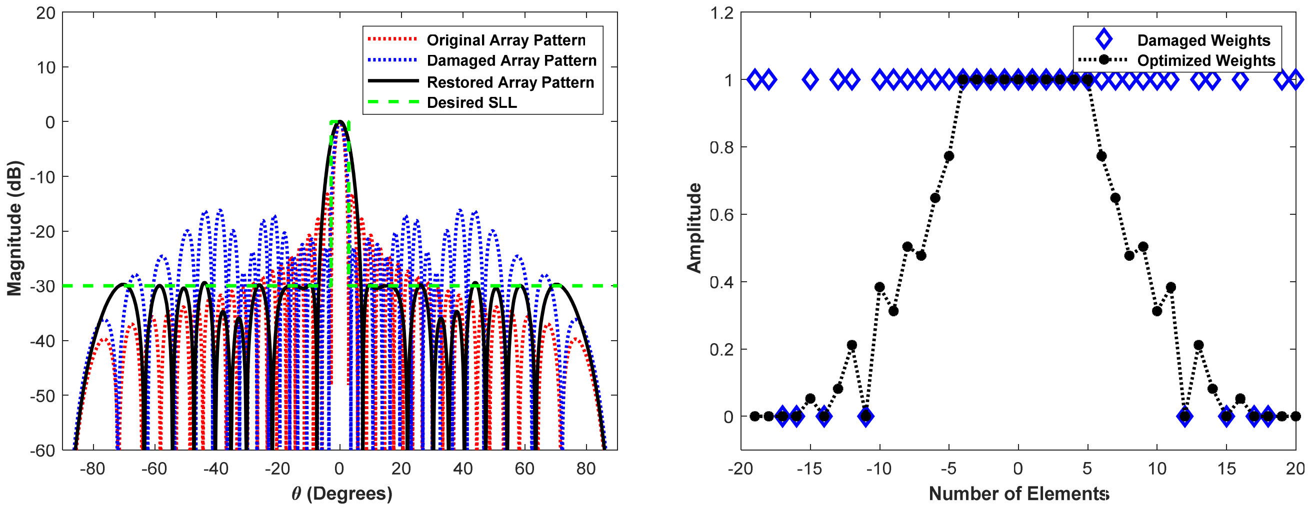

Figure 6. The original, damaged and the restored array patterns and their corresponding amplitude weights for uniform array with 8 defective elements.

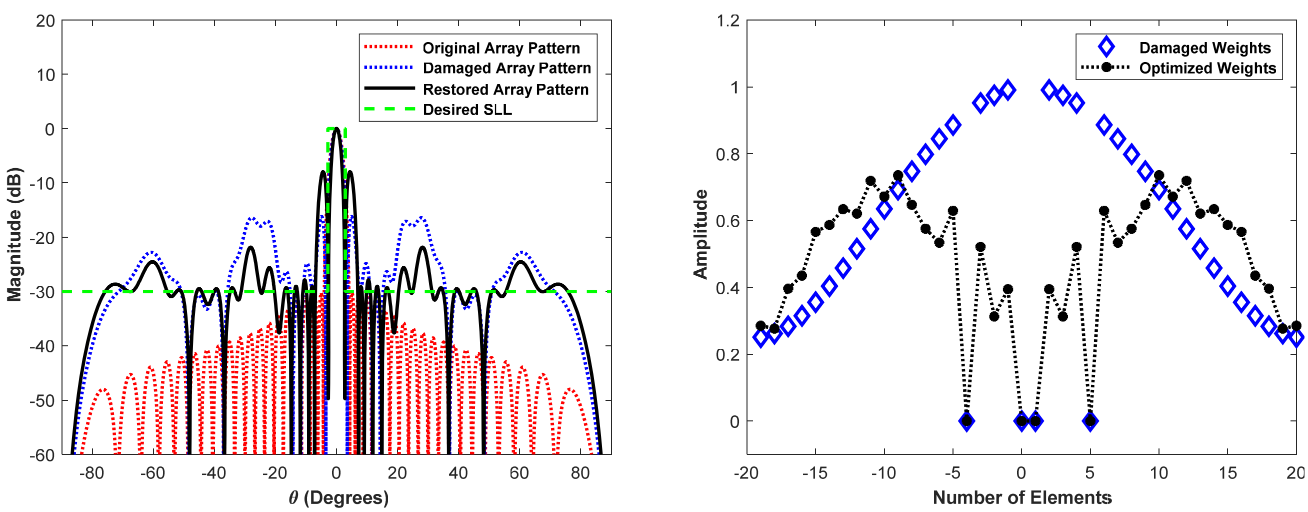

Figure 7. The original, damaged and the restored array patterns and their corresponding amplitude weights for 4 defective elements at the array center.

shows the performance measures for these two cases. It can be observed that the main beam widths of the damaged pattern as well as the restored pattern are not changed greatly with respect to that of the original pattern. This is mainly because the antenna aperture at both array sides does not face any changes. Thus, the effects of the central defective elements have mainly appeared on the very high sidelobes. Note that even if all the other active elements are made optimizable, they cannot compensate for the central defective elements. In order to restore the damaged pattern in such a critical case, it is advised to either replace the hardware of the failed elements or use an automatic RF switch to alter the signal of the defective element to any vicinity active element near the array center.

Finally, the method was extended and applied to the planar array where the number of randomly defective elements was chosen to be 30%. The results are shown in Fig. 9. The compensated elements were able to restore the damaged array patterns successfully in both azimuth and elevation planes.

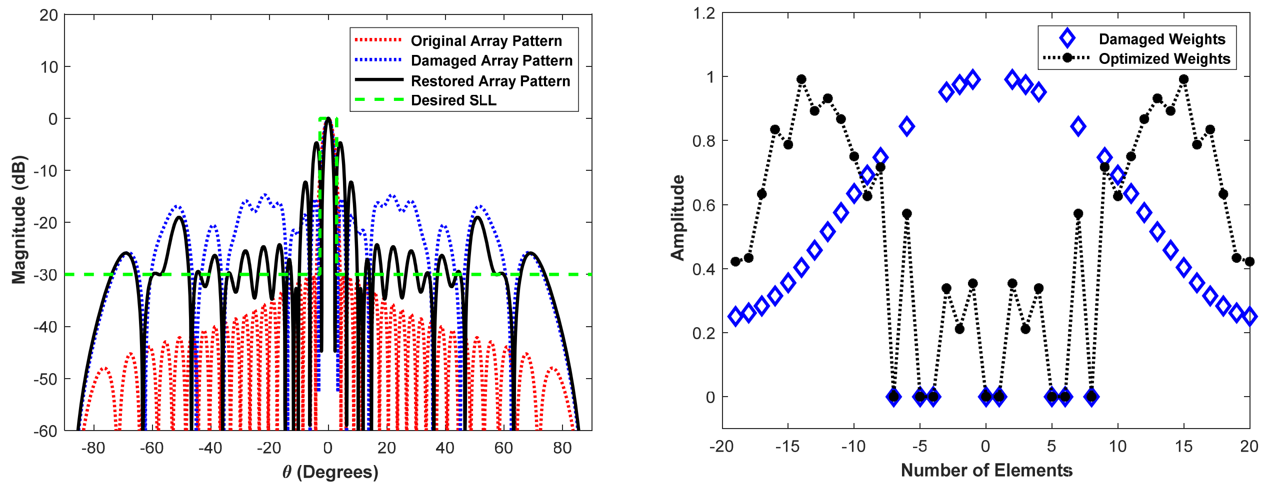

Figure 8. The original, damaged and the restored array patterns and their corresponding amplitude weights for 8 defective elements at the array center.

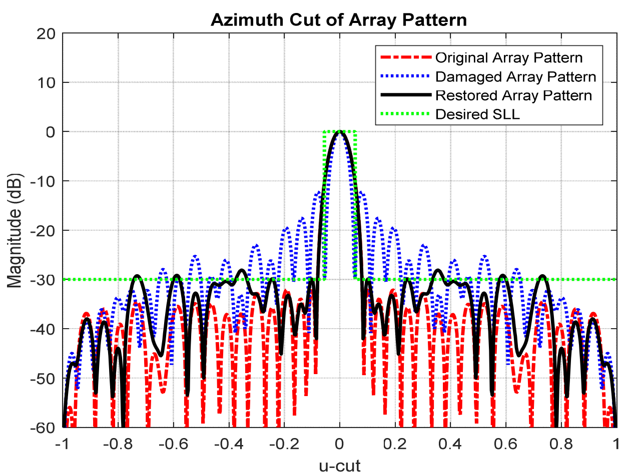

(a)

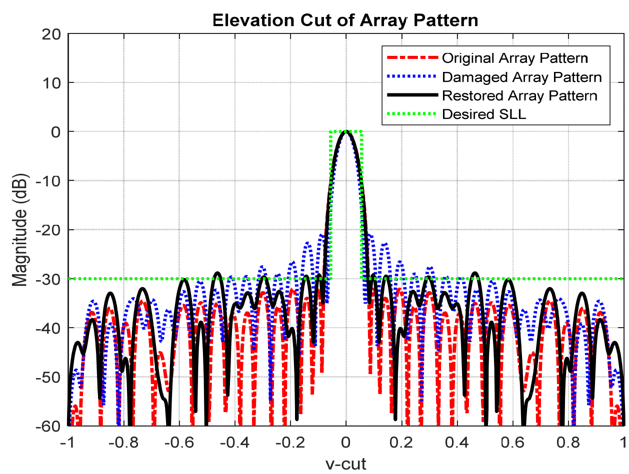

(b)

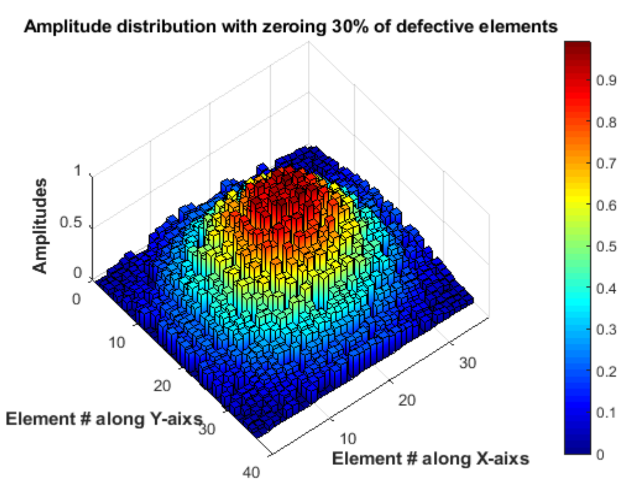

(c)

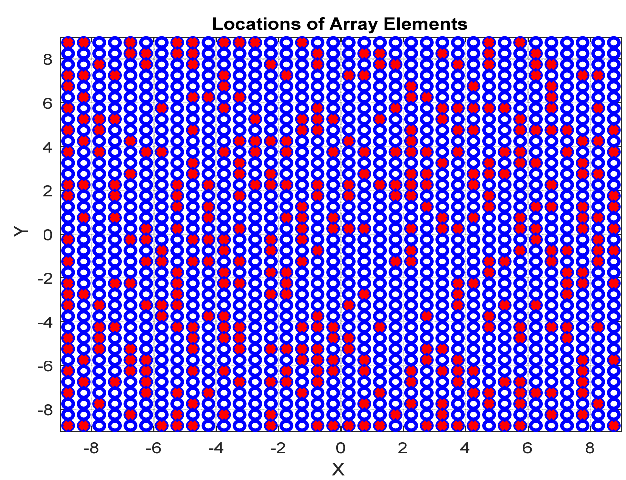

(d)

Figure 9. The original, damaged and the restored array patterns for (a) azimuth plane, (b) elevation plane, their amplitude weights with (c) 30% randomly defective elements, and (d) defective element locations highlighted in red color.

4. CONCLUSIONS

In many practical applications of the phased arrays, the problem of defected elements could not be avoided due to the full long-time operation requirement. All the array elements are randomly and equally vulnerable to such damage problems. This includes the central elements where the excitation amplitudes possess the largest weights that are difficult to rectify. From the obtained results of simulating different scenarios, the following observations can be drawn.

The defective elements at the sides of the array can be easily compensated, and the damaged pattern can be corrected by optimizing all or just a selected number of the array elements. In this case, the directivity, beam width, and the taper efficiency degrade, while the peak SLL can be controlled within the desired level. On the other hand, when the defective elements are at the array center, the SLL cannot be controlled. Suggestions include the hardware replacement of the failed elements or the use of an automatic RF switch to alter the signal of the defective element to any vicinity working element.

REFERENCES

1. Anselmi, N., L. Manica, P. Rocca, and A. Massa, "Tolerance analysis of antenna arrays through interval arithmetic," *IEEE Trans. Antennas Propagat.*, Vol. 61, No. 11, 5496–5507, Nov. 2013, doi: 10.1109/TAP.2013.2276927.
2. Peters, T. J., "A conjugate gradient-based algorithm to minimize the sidelobe level of planar arrays with element failures," *IEEE Trans. Antennas Propagat.*, Vol. 39, 1497–1504, Oct. 1991.
3. Yeo, B.-K. and Y. Lu, "Array failure correction with a genetic algorithm," *IEEE Trans. Antennas Propagat.*, Vol. 47, No. 5, May 1999.
4. Grewal, N. S., M. Rattan, and M. Patterh, "A linear antenna array failure correction using firefly algorithm," *Progress In Electromagnetics Research M*, Vol. 27, 241–254, 2012.
5. Acharya, O. P., A. Patnaik, and S. N. Sinha, "Limits of compensation in a failed antenna array," *International Journal of RF and Microwave Computer-Aided Engineering*, Vol. 24, No. 6, 635–645, 2014.
6. Rodriguez, J. A., F. Ares, E. Morcno, and G. Franceschetti, "Genetic algorithm procedure for linear array failure correction," *Electronics Letters*, Vol. 36, No. 3, Feb. 2000.
7. Mailloux, R. J., "Array failure correction with a digitally beamformed array," *IEEE Trans. Antennas Propagat.*, Vol. 44, 1543–1550, Dec. 1996.
8. Keizer, W. P. M. N., "Element failure correction for a large monopulse phased array antenna with active amplitude weighting," *IEEE Trans. Antennas Propagat.*, Vol. 55, No. 8, Aug. 2007.
9. Mohammed, J. R., "Thinning a subset of selected elements for null steering using binary genetic algorithm," *Progress In Electromagnetics Research M*, Vol. 67, 147–157, 2018.
10. Mohammed, J. R., "A method for thinning useless elements in the planar antenna arrays," *Progress In Electromagnetics Research Letters*, Vol. 97, 105–113, 2021.
11. Balanis, C. A., *Antenna Theory, Analysis and Design*, 4th Edition, Wiley, 2016.
12. Mohammed, J. R., "Optimal null steering method in uniformly excited equally spaced linear array by optimizing two edge elements," *Electronics Letters*, Vol. 53, No. 13, 835–837, Jun. 2017.